Two Shank-Mounted IMUs-Based Gait Analysis and Classification for Neurological Disease Patients

Lei Wang, Yun Sun, Qingguo Li, Tao Liu, *Senior Member, IEEE*, and Jingang Yi, *Senior Member, IEEE*

***Abstract*—Automatic gait measurement and analysis is an enabling tool for intelligent healthcare and robotics-assisted rehabilitation. This letter proposes a novel two shank-mounted inertial measurement units (IMU)-based method on gait analysis and classification for three different neurological diseases. The IMU-based gait analysis and design aims to be applied in personal daily activities and environment for remote diagnosis and rehabilitation guidance. In the design, eight spatial-temporal and kinematic gait parameters are extracted from two shank-mounted IMUs. A support vector machine-based classifier is developed to classify four types of gait patterns with different neurological diseases (healthy control, peripheral neuropathy, post-stroke and Parkinson's disease). A total of 49 subjects are recruited and 93.9% of them are assigned to the right group after the leave-one-subject-out cross validation. The results demonstrate that the proposed IMU-based gait parameters and classifier are capable of differentiating the four types of gait patterns. The analysis and design have great potentials for use in clinical applications.**

***Index Terms*—Medical robots and systems, human-centered automation, gait detection and classification, healthcare automation.**

I. Introduction

GAIT disturbance is a common symptom in various neurological diseases such as post-stroke and Parkinson's disease. Gait analysis and classification is often used as a clinical tool for detecting and diagnosing these diseases [1]. With emerging machine learning techniques, automatic gait classification and disease diagnosis becomes an active research area in the field of intelligent healthcare and automation [2]. Automatic gait classification is important for understanding and extracting the main characteristics of the gait disturbance and therefore benefits the developments of healthcare automation technology [2] and robotics-assisted gait rehabilitation [3], [4].

Motion capture systems and force platforms are typical equipment for automatic gait analysis in laboratory settings. Various gait parameters measured by these systems, including spatial-temporal parameters (e.g., stride length and cadence), kinematic parameters (e.g., range of motion of lower-limb segments and joints), and kinetic parameters (e.g., moments of lower-limb joints), have been considered for determining abnormalities in gait pattern and used for automatic gait classification [5], [6]. Gait analyses of healthy individuals and patients with neurological diseases (e.g., post-stroke [6], [7], Parkinson's disease [8], hereditary spastic paraplegia, cerebral palsy [9] and cruciate ligament deficient [2]) or the same disease in different stages [10], [11] have been studied and reported. Many machine learning-based methods such as artificial neural networks [11], cluster analysis [10] and support vector machine (SVM) [12] are used in these gait detection and diagnosis studies and the reported results achieve high classification accuracy varying from 91.3% to 98% [2], [7], [8], [10]–[12].

Although motion capture systems and force platforms provide adequate and high-precision measurements, they are inconvenient to monitor human motion in personal daily activities and environment due to their high cost and restricted usage spaces. Wearable inertial measurement unit (IMU) is a newly-developed alternative tool for gait analysis in personal daily activities [1], [13]. Various studies have been developed using IMUs on lower limbs to estimate spatial-temporal and kinematic parameters of gait [14]. The cyclic patterns of angular velocity and acceleration measured by IMUs are often used for detecting gait events to extract temporal parameters including gait phase duration and cadence [15]. Pendulum models [15]–[17] and integration of angular velocity and acceleration [18] are used to estimate the motion of lower limbs to extract spatial parameters including walking speed and stride length, and kinematic parameters including the motion ranges of lower-limb joints and segments [14]. These IMU-based gait parameters have been widely applied in clinical studies, to evaluate the gait disturbance [19], [20] and characterize the gait pattern [21], [22] of neurological diseases. Some of them have even been used for the human-robot interactions in robotic assistive devices to help the devices adapting to the patient's motion and gait [23], [24].

A few studies also used IMUs for differentiating and classifying gait types caused by different neurological diseases. Table I summarizes the major IMU-based gait classification

Manuscript received September 11, 2019; accepted January 17, 2020. Date of publication January 31, 2020; date of current version February 11, 2020. This letter was recommended for publication by Associate Editor Massimiliano Zecca and Editor Pietro Valdastri upon evaluation of the reviewers' comments. This work was supported in part by the National Natural Science Foundation of China under Grant 51775485, and in part by the Zhejiang Provincial Natural Science Foundation of China under Grant LZ20E050002. *(Corresponding author: Tao Liu.)*

L. Wang and T. Liu are with the State Key Laboratory of Fluid Power and Mechatronic Systems, School of Mechanical Engineering, Zhejiang University, Hangzhou 310027, China (e-mail: wanglei_me@zju.edu.cn; liutao@zju.edu.cn).

Y. Sun is with the Department of Rehabilitation Medicine, the First Affiliated Hospital, Zhejiang University, Hangzhou 310009, China (e-mail: 1514029@zju.edu.cn).

Q. Li is with the Department of Mechanical and Materials Engineering, Queen's University, Kingston, ON K7L 3N6, Canada (e-mail: ql3@queensu.ca).

J. Yi is with the Department of Mechanical and Aerospace Engineering, Rutgers University, Piscataway, NJ 08854 USA (e-mail: jgyi@rutgers.edu).

Digital Object Identifier 10.1109/LRA.2020.2970656

TABLE I
EXISTING STUDIES ON IMU-BASED CLASSIFICATION

Study	Setting of IMUs	Types of gait	Features	Classifiers	Accuracy
Mannini et al., 2016 [25].	Three IMUs on both shanks and lumbar spine.	Healthy elderly, post-stroke and Huntington's disease.	6 Hidden Markov Models features; 12 time- and frequency-domain features of IMU measurements.	SVM.	90.5%.
Hsu et al., 2018 [26].	Several combinations of seven IMUs attached on lower limbs and trunk.	Post-stroke and other neurological disorders.	192 time-domain features of IMU measurements and 17 gait temporal features in total.	Testing the performance of five classifiers.	89.1% (the highest) when using two IMUs on shanks and Decision Tree classifier.
Caramia et al., 2018 [14].	Several combinations of eight IMUs attached on lower limbs and trunk.	Healthy and three different stages of Parkinson's disease.	87 features in total extracted from 8 spatial-temporal and kinematic gait parameters.	Testing the performance of six classifiers.	96% (the highest) when using all eight IMUs and majority voting of these classifiers.
Sejdic et al., 2014 [27].	One 3D accelerometer on lower back.	Healthy, Parkinson's disease and peripheral neuropathy.	35 time- and frequency-domain features of acceleration.	No classifier, analyzing p-values.	Not reported.

studies for various diseases. Different with the motion capture system-based studies that used the gait parameters for classification, time- and frequency-domain features of IMU measurements are often proposed and used in these approaches [25]–[27]. It is maybe more convenient to extract these time- and frequency-domain features than to estimate the gait parameters by the IMU measurements. These features can be used to classify the different gait types with an accuracy of about 90%. However, it is challenging to build relationship between these time- and frequency-domain features from IMUs with actual gait disturbances and then to characterize gait patterns of patients with diseases. This shortcoming would reduce the clinical application value by using wearable IMUs. Hsu *et al.* [26] combined some temporal gait parameters for gait classification. However, the lack of spatial and kinematic parameters in the approach would cause the incompleteness to describe the gait pattern. Caramia *et al.* [14] estimated various spatial-temporal and kinematic gait parameters from eight IMUs on the lower-limb segments and the trunk for gait classification, and obtained a high accuracy of 96%. However, the large amount of IMUs would cause inconvenience and discomfort in personal daily activities.

The goal of this study is to propose and validate a novel method to characterize and classify different gait types by using only two shank-mounted IMUs. The main advantage of the approach lies in its easy and convenience usage in personal daily activities and environments for remote diagnosis and robotics-assisted gait rehabilitation. In this study, gait parameters are estimated by the two IMUs to characterize the gait patterns. Because of the limited measurements of the two IMUs, most kinematic parameters used in the existing works (e.g., the ranges of lower-limb joint rotation [5], [14]) cannot be estimated and obtained. Instead, a novel set of five kinematic parameters are proposed and estimated to capture the key characteristics of the linear ankle motion and shank rotation. As ankle and shank are on the distal part of lower limbs, most of the dysfunctions of lower-limb segments and joints would cause the deviations of ankle and shank motion [28]. The new set of kinematic parameters provides valuable information to detect the gait abnormalities. We also estimate three spatial-temporal gait parameters that are commonly used in previous gait evaluation studies [19], [20]. This work recruits four groups of subjects, including healthy control group and three patients groups with peripheral neuropathy, post-stroke and Parkinson's diseases, respectively. The proposed eight gait parameters are used to characterize the gait pattern of each group. A SVM-based classifier is developed to classify the four types of gait patterns. Leave-one-subject-out cross validation [25] and statistical analysis are also implemented to validate the performance of the proposed method. The proposed approach can be extended for real-time gait diagnosis and classifitication and further integrated with robotics-assisted rehabilitation applications.

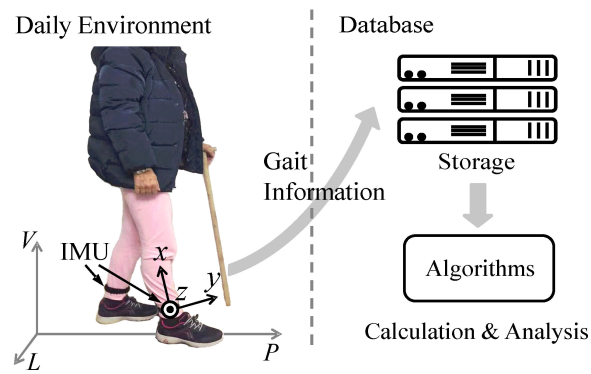

Fig. 1. The proposed system for gait classification.

II. METHOD

A. Gait Detection Sensing System

Fig. 1 shows the system used in this study for gait classification. Two IMUs (InvenSense MPU-6050, including a 3D accelerometer with a range of $\pm$8g and a 3D gyroscope with a range of $\pm$1000°/s) are used in the system. Each IMU was attached close to the ankle on each shank and positioned in the shank sagittal plane on the lateral side. The x-axis of each IMU was along the shank in the sagittal plane; the y-axis was in the anterior-posterior direction to the shank in the sagittal plane; and the z-axis was in the mediolateral direction to the shank and perpendicular to the sagittal plane. For the convenience of

TABLE II
INFORMATION OF PARTICIPANTS

Group	Number of subjects	Height [a] (m)	Weight [a] (Kg)	Age [a] (year)	Gender
HC	13	1.67 ± 0.11	67 ± 12	49 ± 20	7 males, 6 females
PN	8	1.64 ± 0.04	57 ± 4	40 ± 8	3 males, 5 females
PS	13	1.69 ± 0.10	71 ± 16	61 ± 15	9 males, 4 females
PD	15	1.63 ± 0.08	61 ± 11	76 ± 7	9 males, 6 females

[a]Mean ± S. D.

defining gait parameters, a global coordinate system was also defined. The P-axis of the global coordinate system is along the direction of progression; the V-axis is along the direction of gravity; and the L-axis is in the medio-lateral direction. The IMU measurements were sampled and collected at a frequency of 100 Hz. A database sub-system was built to store and analyze the collected data.

B. Participants and Protocols

The subject groups in this study include eight patients with peripheral neuropathy (PN) caused by n-hexane, thirteen patients with post-stroke (PS), fifteen patients with Parkinson's disease (PD), and thirteen healthy controls (HC). The three types of diseases were selected primarily for their impacts on clinical significance and also their different clinical symptoms in gait patterns caused by different nervous system disorders [20], [26], [27]. The inclusion criteria of the patients were their obvious gait disturbances that were evaluated and determined by therapists. These patients can walk independently and the healthy controls did not report to have any dysfunction in motor system. Table II lists the information of each group of subjects. All subjects gave their informed consent for inclusion before they participated in the study. This study was approved by the Medical Ethics Committee of School of Medicine at Zhejiang University [29]. The project identification code is 2018-005.

The participants were asked to walk straight in preferred speed with the IMUs for more than 12 meters on a flat floor. For each participant, the proposed gait parameters were estimated by the IMU measurements for the middle ten steps under steady walking state in the walking trial. These data and estimation were used for training and validating the proposed gait classifier. All the participants were included in the further analysis.

As a preliminary clinical application, seven of the PN subjects were tested another time by the developed classifier after they have recovered from neuropathy and are going to be discharged from hospital.

C. Gait Parameters Used for Classification

Eight gait parameters were proposed in this study to characterize the gait pattern. These gait parameters were estimated in each gait cycle based on methods developed in [15], [16] and [30]. Heel-strike and toe-off gait events were firstly detected according to the cyclic pattern of z-axis angular velocity of the shank-mounted IMU using the method in [15]. Heel-strikes were used to separate the trial into gait cycles. Toe-off was used to separate gait cycle into swing phase and stance phase. The next step is calculating the motion trajectory of IMU during each gait cycle by the integration of angular velocity and acceleration [18], [30]. To reduce accumulated error due to integration, zero velocity state of the ankle motion was detected and compensations were calculated in each stance phase for resetting and correcting the IMU's motion [30]. The ankle motion trajectory was then calculated from the trajectory of IMU by the relative position between them. To avoid the influence of the IMU location variation among the subjects, during each gait cycle the P-axis (progression direction) of the global coordinate system (Fig. 1) was reset as along the connection between the last and the newly calculated landing points of the ankle. The corresponding L-axis (medio-lateral direction) was also reset.

Based on the detected gait phases and calculated motion trajectories, three spatial-temporal gait parameters and five kinematic gait parameters were extracted and these eight parameters are listed and described as follows.

1) Stride length (SL): the linear displacement between two adjacent landing points.
2) Gait cycle duration (GD): the duration between two adjacent heel-strike events.
3) Percentage swing phase (PSP): the duration between adjacent toe-off event and heel-strike event divided by GD.
4) Max ankle velocity (MV): the maximum value of ankle velocity in P-axis (Fig. 1) direction during the gait cycle.
5) Max ankle height (MH): the maximum value of ankle displacement in V-axis direction during the gait cycle.
6) Ankle horizontal displacement at MH (MHD): the ankle displacement in P-axis direction when MH occurs.
7) Range of shank motion (RS): the range of the integration of IMU z-axis angular velocity during swing phase.
8) Kinematic Asymmetry (KS): a parameter that describes the asymmetry between the motion of human left side and right side. KS was calculated as

$$KS = \sqrt{\sum\nolimits_{i=3}^{7} \left(\frac{\Delta_i}{\sigma_i}\right)^2} \tag{1}$$

where Δ_i is the difference of the *i*th gait parameter between two continuous steps of left side and right side; σ_i is the standard deviation of the *i*th gait parameter in the steps from healthy subjects.

Considering their dependences on subject's biomechanical parameters, gait parameters SL, MV, MH and MHD were normalized and divided by subject's height. Some subjects have severe asymmetry of the left-side and right-side motions and this would cause the great differences among left-side and right-side gait parameters. Thus, except the asymmetry parameter KS, the rest seven parameters used in the classifier training and validating were all the average value of the current step and the following step on the other side.

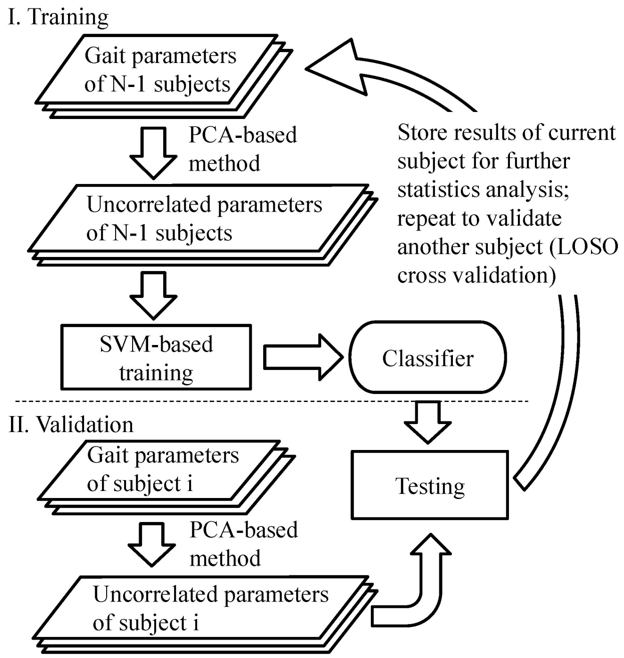

Fig. 2. Process schematic of training and validation of the proposed classifier.

D. SVM-Based Classifier

A SVM-based classifier was developed to classify the four different types of gait patterns. Ten walking steps were collected in each subject, and each step was classified independently. Leave-one-subject-out (LOSO) cross validation [25] was performed. This implies that for the validation of each subject, the 480 steps from the rest 48 subjects were used for training a classifier and the 10 steps of this subject were used for testing the classifier. An algorithm was developed and implemented in MATLAB (MathWorks, Inc., Natick, MA, USA) for the training and validation process. Fig. 2 illustrates the process schematic of the algorithm.

The basic principle of the classifier was to differentiate the abnormities in gait pattern among the four subject groups. The normal range of gait pattern was defined by the gait parameters of healthy group in the training dataset. As intrinsic correlation exists among these eight parameters in healthy group, a simple calculation of the abnormality of each gait parameter cannot reflect the abnormal relationship [31]. Thus, a principal component analysis-based method was applied in this study. This method would determine the intrinsic underlying correlation among the eight gait parameters, and produce a new set of uncorrelated parameters from the original parameters set. The new parameters set indicates the abnormalities of both the gait parameters and their relationships. In the following, we briefly describe this method.

The gait parameters were firstly standardized as

$$z_i = (x_i - \mu_i)/\sigma_i \tag{2}$$

where x_i is the *i*th origin gait parameter; z_i is the *i*th standardized gait parameter; and μ_i, σ_i are the mean and standard deviation of the *i*th gait parameter of healthy steps in the training dataset, respectively. The standardization eliminates the impact of the different scales among these parameters. A covariance matrix of the standardized gait parameters of healthy steps and its eigenvalue–eigenvector pairs were then calculated. Based on the eigenvalue–eigenvector pairs, a new set of uncorrelated parameters were calculated as

$$y_i = \frac{1}{\sqrt{\lambda_i}} z \cdot \alpha_i \tag{3}$$

where λ_i and α_i are the *i*th eigenvalue–eigenvector pair, respectively, y_i is the *i*th new parameter, and z is the set of z_i.

The next step is to train SVMs with the new set of parameters. One SVM was trained for distinguishing the data points of one group of subjects from the other groups. Thus four SVMs were trained for the four groups in total. The SVM library of MATLAB R2014a [32] was applied for the SVM solver. Linear kernel function and Sequential Minimal Optimization (SMO) method were used during the training process.

The final step is to assign the data points of testing dataset into the four groups. For each group, the separating hyperplane of SVM is expressed as

$$w \cdot y + b = 0 \tag{4}$$

where w is an eight-dimension coefficient of the function, y is the set of uncorrelated parameters given by (3), and b is the bias vector. The distance d of a data point away from the SVM hyperplane is calculated as

$$d = (w \cdot y_0 + b) / \|w\| \tag{5}$$

where y_0 is the set of uncorrelated parameters of the data point, and $\|w\|$ is the norm of w. The positive value of the distance indicates that the data point is in the range of the corresponding group. A larger distance value means the larger possibility of the data point being assigned in the group. To finally assign the data point, the distances of the data point away from the four SVM hyperplanes of the four groups were compared and the data point was assigned in the group with the largest computed distance.

E. Statistics Analysis

To present the extent of the difference in gait pattern between patient groups and healthy group, a normalcy index (NI) developed in [31] is introduced and calculated as a metric for each subject. The NI is the Euclidean distance between the sets of uncorrelated parameters of the patient and the healthy mean (zero point)

$$NI = \sqrt{\sum\nolimits_{i=1}^{8} y_i^2} \tag{6}$$

The higher NI value means the greater abnormality of gait pattern.

The proposed classifier contained four SVMs, and each SVM was used to distinguish the steps in one group from the steps not in the group. To validate the performance of each SVM, sensitivity and specificity [22] were calculated as

$$Sensitivity = TP/P \tag{7}$$

$$Specificity = TN/N \tag{8}$$

where *P* and *N* are the total number of steps from the group and not from the group respectively, *TP* is the number of the steps that were in the group and correctively assigned by the SVM, and *TN* is the number of the steps that were not in the group and correctively assigned by the SVM.

To validate the overall performance of the proposed classifier, the overall accuracy on classifying the individual steps into the four groups is calculated as

$$Accuracy_{step} = T_{st}/A_{st} \cdot 100\% \tag{9}$$

where T_{st} is the number of the correctly classified steps and A_{st} is the total number of steps of all subjects. To validate the classification accuracy of each group, a confusion matrix is implemented and lists the detailed results of correct classifications and misclassifications in each group [25].

Majority voting is applied for analyzing the performance of the proposed classifier on classifying the subjects into the four groups [25]. This implies that a subject would be classified into the group where the majority steps of the subject are assigned. When a tie exists, the subject would be classified into the group with the larger mean value of the distance calculated by (5). The overall accuracy on subject classification was calculated as

$$Accuracy_{subject} = T_{su}/A_{su} \cdot 100\% \tag{10}$$

where T_{su} is the number of the correctly classified subject and A_{su} is the total number of subjects. A confusion matrix is also implemented.

The influence of the gait parameters estimation errors on the classification accuracy needs to be investigated. The estimation accuracy of parameter GC and PSP depends on the accuracy of detecting heel-strike event and toe-off event. A previous study showed that the mean error of the method applied in this study on detecting heel-strike and toe-off were -14 and 23 ms respectively [33]. The estimations of parameter SL, MV, MH and MHD have been validated by seven PN subjects with a motion capture system (T40S, Vicon Motion Systems Ltd., UK) in our pervious study. The root-mean-square errors were 2.3 cm for SL, 3.0 cm/s for MV, 1.0 cm for MH and 1.9 cm for MHD. To quantify the influence of each estimation error, the reported error is used to the proposed classifier by adding the value of error on the corresponding parameter in testing dataset. The change in overall classification accuracy is finally calculated.

III. Results and Discussions

A. Results

Fig. 3 shows the differences on distribution of each gait parameter among the four groups. The NIs calculated by (6) were 3.7 ± 0.7 (mean ± S. D.) in HC group, 9.0 ± 1.0 in PN group, 21.7 ± 16.0 in PS group and 7.4 ± 3.7 in PD group.

The sensitivities and specificities of the four SVMs contained in the proposed classifier are shown in Table III. The overall accuracy on classifying individual steps into the four groups is 87.8%. After the majority voting, the overall accuracy on classifying the subjects into the four groups is 93.9%. Confusion matrixes are used to show the detailed results of the correct classifications and misclassifications. Table IV lists the confusion matrix for the results of individual step classification. Table V lists the confusion matrix for the results of subject classification after the majority voting.

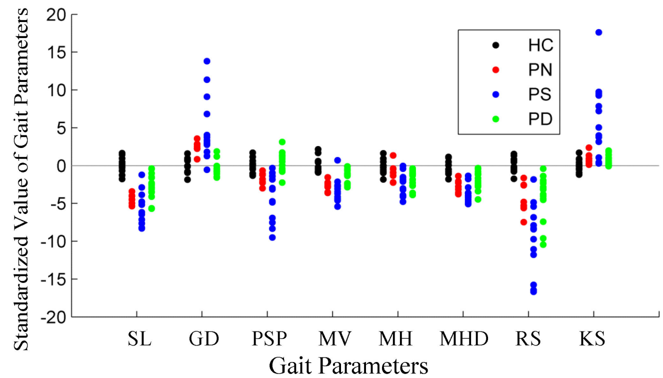

Fig. 3. The distribution of each gait parameter among the four groups: HC, PN, PS and PD. Each point represents the mean value of the gait parameter of a subject. The parameters have been standardized as (2) for the convenience on presentation and comparison.

TABLE III
Sensitivity and Specificity of Each SVM

SVM	Sensitivity	Specificity
HC vs. non-HC	0.900	0.886
PN vs. non-PN	0.788	0.844
PS vs. non-PS	0.800	0.894
PD vs. non-PD	0.933	0.903

TABLE IV
Confusion Matrix of Individual Step Classification

Actual Group	Classification Output HC	PN	PS	PD
HC	**118 (90.8%)**	5 (3.9%)	2 (1.5%)	5 (3.9%)
PN	2 (2.5%)	**62 (77.5%)**	15 (18.8%)	1 (1.3%)
PS	10 (7.7%)	9 (6.9%)	**108 (83.1%)**	3 (2.3%)
PD	3 (2.0%)	3 (2.0%)	2 (1.3%)	**142 (94.7%)**

Each line lists the numbers of the steps (percentages of the steps) in the actual group that were classified into the four groups. Correct classifications are in bold.

We also test the influences of the gait parameters estimation errors on the overall accuracy of individual step classification. The classification accuracy reduces less than 1% after incorporating the reported estimation error of the heel-strike event or MHD into the classifier, and reduces less than 2% after incorporating the estimation error of the toe-off event, SL or MV into the classifier. However, 5.6% reduction of classification accuracy was resulted after incorporating the reported estimation error of MH.

Seven of the PN subjects were tested later by the developed classifier after they have recovered from neuropathy and are going to be discharged from hospital. Six of them were successfully classified into healthy group.

TABLE V
CONFUSION MATRIX AFTER MAJORITY VOTING

Actual Group	Classification Output HC	PN	PS	PD
HC	**12 (92.3%)**	1 (7.7%)	0 (0.0%)	0 (0.0%)
PN	0 (0.0%)	**7 (87.5%)**	1 (12.5%)	0 (0.0%)
PS	1 (7.7%)	0 (0.0%)	**12 (92.3%)**	0 (0.0%)
PD	0 (0.0%)	0 (0.0%)	0 (0.0%)	**15 (100%)**

Each line lists the numbers of the subjects (percentages of the subjects) in the actual group that were classified into the four groups. Correct classifications are in bold.

B. Discussions

In this study, a novel method on classifying different types of gait by two shank-mounted IMUs was proposed and validated. In total of 49 subjects divided into four groups (HC, PN, PS and PD) were recruited. The overall accuracy of the proposed method on individual step classification reached to 87.8% with the LOSO cross validation. After majority voting of the classification results of the steps, 93.9% of the subjects were classified into the right group. This indicated that the proposed method is capable of differentiating between the four types of gait.

Compared with the existing studies [2], [7], [8], [10]–[12] that used the parameters measured by motion capture systems or force platforms for gait classification, less gait information was used in this study because of the small number of used IMUs. The approach has attractive features such as light-weight, low-cost, non-intrusive for human movement and personal daily activities. Even using less information, the proposed classifier obtained an accuracy of 93.9%, which reached a similar level to those in the above-mentioned studies (91.3% to 98% accuracy).

The previous studies [14], [25]–[27] have used IMUs for classifying many different types of gait patterns (see Table I). Time- and frequency-domain features of IMU measurements were proposed and used in many studies [25]–[27]. These features classified the different types of gait with accuracy of about 90%. However, few of them are applied for gait analysis in clinical studies due to the difficulty of relating them with the actual gait disturbances and to characterize gait patterns of different diseases. The three spatial-temporal parameters used in this study have been applied in clinical gait analysis and the remaining five kinematic parameters quantified the motion deviations of lower limbs. Compared with the time- and frequency-domain features, the proposed set of gait parameters provides additional clinical application value.

Hsu *et al.* [26] also used several temporal gait parameters for the classification and reached an accuracy of 89.1%. Compared with the results in [26], additional spatial and kinematic parameters were used here for describing the gait pattern, and a higher accuracy (93.9%) was obtained. Caramia *et al.* [14] used many spatial-temporal and kinematic gait parameters extracted from eight IMUs for gait classification and reached a high accuracy of 96%. Compared with the approach in [14], only two shank-mounted IMUs were used in this work, which improves the applicability for personal daily activities. The set of kinematic parameters in this work was newly developed and was extracted from the linear ankle motion and shank rotation. Most of the dysfunctions of lower-limb segments and joints can cause the deviations of ankle and shank motion [28] and our development was inspired by this observation. Four types of patient gaits were classified in this study by the same set of gait parameters and this is new compared with the existing studies [14], [25]–[27]. In addition, Fig. 3 showed the differences on distribution of the proposed eight gait parameters among the four groups. Each type of gait pattern showed its own characteristics on the distribution of the eight gait parameters. All of the comparison results indicate the superior performance and attractive features of the proposed approach than the existing methods.

The study has good potential for further applications. As a preliminary application in this study, seven PN subjects took a second test by the proposed classifier after they have recovered, and six of them were successfully assigned into healthy group. This indicates the potential application in the area of intelligent diagnosis. The proposed IMU system can be also applied for robotic devices on walking assistance and rehabilitation training. The automatically calculated gait pattern and classification information can help these devices adapting to patient's gait and designing personalized rehabilitation [4], [34]. In addition, the proposed classifier can extract targeted index for evaluating a certain type of gait. NI calculated by (6) was used as a single metric to quantity the extent of a patient's gait deviating from healthy gait. However, as mutual scope of NI existed among different patient groups, it is challenging to only use NI to distinguish and diagnose these patients. This work showed that the characteristics of a gait pattern caused by the disease can be quantified by the distance to corresponding hyperplane calculated by (5). Comparing with NI, this distance can be regarded as a more sensitive and targeted index for the gait evaluation and identification. It could be applied in many clinical applications such as providing treatment feedback and assessing the probability of suffering a disease.

Although the proposed gait parameters showed good performance to differentiate the four gait types, the selection of gait parameters still deserves further studies. As shown in Tables III to V, there exist some misclassifications. The most severe one was that 18.8% of the steps from PN group were assigned into the PS group. This indicated that additional gait information was required for differentiating gaits of PN and PS. The influences of the gait parameters estimation errors on the classification accuracy were tested in this study. Most of the estimation errors did not produce any significant influence on classification except that the estimation error of MH caused a large accuracy reduction (5.6%). The MH should be considered for being replaced by other alternative parameters that contain the similar information but can be estimated precisely. Several previous studies include the variance of the parameters as features in the classification, with the consideration that the patient walking gait is more unstable than healthy people [14]. The variance parameters would be considered in further study to improve the current classification accuracy. The time- and frequency-domain features in [25]–[27] would also be considered and combined with the proposed gait parameters in this study to provide additional information for the classification.

There were some other limitations in this work. Even though the subjects in a group have the same type of disease, their impairments in nervous system can be different. This would cause different sub-types of gait patterns [11]. However, no sub-group was set in this study. In addition, the clinical evaluations by therapists were missing. They are important for evaluating the actual motor system disorders by clinical symptoms and these evaluations are helpful for understanding the scope of work of the proposed classifier.

IV. Conclusion

This study proposed a novel method on classifying four types of gait (HC, PN, PS and PD) with two shank-mounted IMUs. A new set of eight gait parameters estimated by the IMUs was proposed for characterizing the gait pattern under each type of disease. Using the two IMUs, a SVM-based classifier was developed for the gait analysis and classification. Although less IMUs were used and more types of gait were classified compared with previous studies, the proposed gait parameters and classifier showed a good performance on classifying the four gait types with a similar level of classification accuracy (overall accuracy 93.9%) to the existing studies. The approach has great potentials for further applications on intelligent diagnosis, healthcare automation and robotics-assisted rehabilitation. Future work would be focusing on extending the set of gait parameters to reduce the misclassifications and improve the classification accuracy.

References

[1] S. S. Chen, J. Lach, B. Lo, and G. Z. Yang, "Toward pervasive gait analysis with wearable sensors: A systematic review," *IEEE J. Biomed. Health Informat.*, vol. 20, no. 6, pp. 1521–1537, Nov. 2016.

[2] W. Wu, W. Zeng, L. M. Ma, C. Z. Yuan, and Y. Zhang, "Modeling and classification of gait patterns between anterior cruciate ligament deficient and intact knees based on phase space reconstruction, Euclidean distance and neural networks," *BioMed. Eng. OnLine*, vol. 17, Nov. 2018, Art. no. 165.

[3] J. Lanini, H. Razavi, J. Urain, and A. Ijspeert, "Human intention detection as a multiclass classification problem: application in physical human-robot interaction while walking," *IEEE Robot. Automation Lett.*, vol. 3, no. 4, pp. 4171–4178, Oct. 2018.

[4] G. Chalvatzaki, X. S. Papageorgiou, P. Maragos, and C. S. Tzafestas, "Learn to adapt to human walking: A model-based reinforcement learning approach for a robotic assistant rollator," *IEEE Robot. Automation Lett.*, vol. 4, no. 4, pp. 3774–3781, Oct. 2019.

[5] V. Cimolin and M. Galli, "Summary measures for clinical gait analysis: A literature review," *Gait Posture*, vol. 39, pp. 1005–1010, Apr. 2014.

[6] S. Kinsella and K. Moran, "Gait pattern categorization of stroke participants with equinus deformity of the foot," *Gait Posture*, vol. 27, no. 1, pp. 144–151, Jan. 2008.

[7] B. Pogorelc and M. Gams, "Detecting gait-related health problems of the elderly using multidimensional dynamic time warping approach with semantic attributes," *Multimedia Tools Appl.*, vol. 66, no. 1, pp. 95–114, Sep. 2013.

[8] A. Prochazka, O. Vysata, M. Valis, O. Tupa, M. Schatz, and V. Marik, "Bayesian classification and analysis of gait disorders using image and depth sensors of Microsoft Kinect," *Digital Signal Process.*, vol. 47, pp. 169–177, Dec. 2015.

[9] S. I. Wolf *et al.*, "Gait analysis may help to distinguish hereditary spastic paraplegia from cerebral palsy," *Gait Posture*, vol. 33, no. 4, pp. 556–561, Apr. 2011.

[10] S. Mulroy, J. Gronley, W. Weiss, C. Newsam, and J. Perry, "Use of cluster analysis for gait pattern classification of patients in the early and late recovery phases following stroke," *Gait Posture*, vol. 18, no. 1, pp. 114–125, Aug. 2003.

[11] K. Kaczmarczyk, A. Wit, M. Krawczyk, and J. Zaborski, "Gait classification in post-stroke patients using artificial neural networks", *Gait Posture*, vol. 30, no. 2, pp. 207–210, Aug. 2009.

[12] R. Begg and J. Kamruzzaman, "A machine learning approach for automated recognition of movement patterns using basic, kinetic and kinematic gait data," *J. Biomech.*, vol. 38, no. 3, pp. 401–408, Mar. 2005.

[13] M. Trkov, K. Chen, J. G. Yi, and T. Liu, "Inertial sensor-based slip detection in human walking," *IEEE Trans. Automation Sci. Eng.*, vol. 16, no. 3, pp. 1399–1411, Jul. 2019.

[14] C. Caramia *et al.*, "IMU-based classification of parkinson's disease from gait: A sensitivity analysis on sensor location and feature selection," *IEEE J. Biomed. Health Informat.*, vol. 22, no. 6, pp. 1765–1774, Nov. 2018.

[15] K. Aminian, B. Najafi, C. Bula, P. F. Leyvraz, and P. Robert, "Spatio-temporal parameters of gait measured by an ambulatory system using miniature gyroscopes," *J. Biomech.*, vol. 35, no. 5, pp. 689–699, May 2002.

[16] L. Wang, Y. Sun, Q. Li, and T. Liu, "Estimation of step length and gait asymmetry using wearable inertial sensors," *IEEE Sens. J.*, vol. 18, no. 9, pp. 3844–3851, May 2018.

[17] A. Zijlstra and W. Zijlstra, "Trunk-acceleration based assessment of gait parameters in older persons: A comparison of reliability and validity of four inverted pendulum based estimations," *Gait Posture*, vol. 38, no. 4, pp. 940–944, Sep. 2013.

[18] Q. Li, M. Young, V. Naing, and M. Donelan, "Walking speed estimation using a shank-mounted inertial measurement unit," *J. Biomech.*, vol. 43, no. 8, pp. 1640–1643, May 2010.

[19] A. Salarian *et al.*, "Gait assessment in parkinson's disease: Toward an ambulatory system for long-term monitoring," *IEEE Trans. Biomed. Eng.*, vol. 51, no. 8, pp. 1434–1443, Aug. 2004.

[20] D. Trojaniello *et al.*, "Estimation of step-by-step spatio-temporal parameters of normal and impaired gait using shank-mounted magneto-inertial sensors: application to elderly, hemiparetic, parkinsonian and choreic gait," *J. NeuroEng. Rehabil.*, vol. 11, Nov. 2014, Art. no. 152.

[21] I. Tien, S. D. Glaser, and M. J. Aminoff, "Characterization of gait abnormalities in Parkinson's disease using a wireless inertial sensor system," in *Proc. 32nd Annu. Int. Conf. IEEE Eng. Med. Biol. Soc.*, 2010, pp. 3353–3356.

[22] J. Barth *et al.*, "Biometric and mobile gait analysis for early diagnosis and therapy monitoring in Parkinson's disease," in *Proc. 33rd Annu. Int. Conf. IEEE Eng. Med. Biol. Soc.*, 2011, pp. 868–871.

[23] C. A. Cifuentes, A. Frizera, R. Carelli, and T. Bastos, "Human–robot interaction based on wearable IMU sensor and laser range finder," *Robot. Auton. Syst.*, vol. 62, no. 10, pp. 1425–1439, 2014.

[24] Y. Z. Zhang, K. H. Song, J. G. Yi, P. F. Huang, Z. S. Duan, and Q. J. Zhao, "Absolute attitude estimation of rigid body on moving platform using only two gyroscopes and relative measurements," *IEEE/ASME Trans. Mechatronics*, vol. 23, no. 3, pp. 1350–1361, Jun. 2018.

[25] A. Mannini, D. Trojaniello, A. Cereatti, and A. M. Sabatini, "A machine learning framework for gait classification using inertial sensors: application to elderly, post-Stroke and Huntington's disease patients," *Sensors*, vol. 16, no. 1, Jan 2016, Art. no. 134.

[26] W. C. Hsu *et al.*, "Multiple-wearable-sensor-based gait classification and analysis in patients with neurological disorders," *Sensors*, vol. 18, no. 10, Oct. 2018, Art. no. 3397.

[27] E. Sejdic, K. A. Lowry, J. Bellanca, M. S. Redfern, and J. S. Brach, "A comprehensive assessment of gait accelerometry signals in time, frequency and time-frequency domains," *IEEE Trans. Neur. Sys. Reh.*, vol. 22, no. 3, pp. 603–612, May 2014.

[28] J. Perry, "Ankle and foot gait deviations," in *Gait Analysis: Normal and Pathological Function*, Thorofare, USA: SLACK Inc., 1992, pp. 185–222.

[29] Zhejiang University, "Zhejiang university school of medicine," 2019, [Online]. Available: http://www.cmm.zju.edu.cn/index.php?a=content&catid=90&web=english&pc=1

[30] L. Wang *et al.*, "Inertial sensor-based gait analysis for evaluating the effects of acupuncture treatment in Parkinson's disease," *presented at the IEEE/ASME Int. Conf. on Advanced Intelligent Mechatronics*, Hong Kong, China, Jul. 8-12, 2019, pp. 323–328.

[31] L. M. Schutte, U. Narayanan, J. L. Stout, P. Selber, J. R. Gage, and M. H. Schwartz, "An index for quantifying deviations from normal gait," *Gait & Posture*, vol. 11, pp. 25–31, Feb. 2000.

[32] MathWorks, "Support vector machines 2014a," 2014, [Online]. Available: https://www.mathworks.com/help/releases/R2014a/stats/support-vector-machines.html

[33] J. M. Jasiewicz *et al.*, "Gait event detection using linear accelerometers or angular velocity transducers in able-bodied and spinal-cord injured individuals," *Gait Posture*, vol. 24, no. 4, pp. 502–509, Dec. 2006.

[34] W. G. Huo, S. Mohammed, Y. Amirat, and K. Kong, "Fast gait mode detection and assistive torque control of an exoskeletal robotic orthosis for walking assistance," *IEEE Trans. Robotics*, vol. 34, no. 4, pp. 1035–1052, Aug. 2018.